PHILOSOPHICAL TRANSACTIONS OF THE ROYAL SOCIETY A MATHEMATICAL, PHYSICAL & ENGINEERING SCIENCES

Applications of High-Resolution ^{13}C and ^{15}N n.m.r. of Solids [and Discussion]

J. Schaefer, E. O. Stejskal, M. D. Sefcik, R. A. McKay and G. C. Levy

Phil. Trans. R. Soc. Lond. A 1981 **299**, 593-608
doi: 10.1098/rsta.1981.0037

Phil. Trans. R. Soc. Lond. A **299**, 593–608 (1981)
Printed in Great Britain

Applications of high-resolution ^{13}C and ^{15}N n.m.r. of solids

By J. Schaefer, E. O. Stejskal, M. D. Sefcik and R. A. McKay
Monsanto Company, Physical Sciences Center, 800 N. Lindbergh Boulevard, St Louis, Missouri 63166, U.S.A.

The combination of cross polarization, dipolar decoupling and magic angle spinning results in liquid-like high-resolution ^{13}C and ^{15}N n.m.r. spectra of a wide variety of solid materials. Structural determinations based on such ^{13}C n.m.r. spectra include the measurement of the extent to which pyrolysed polyacrylonitrile fibres (Orlon) retain aliphatic character during the first step of the production of a carbon fibre, the determination of the chemical identity of the cross links formed from an acetylene-terminated polyimide resin, and the characterization of the metabolic products of a bacterial fermentation of wood lignin. All of these non-destructive analyses are performed on intact heterogeneous samples. The high resolution of the carbon experiment can also be exploited by obtaining *proton* spin–lattice relaxation parameters for chemically different protons in solids. Because of spin diffusion, these parameters are dependent on spatial proximity and so are helpful in measuring the homogeneity of solid blends of polymers such as poly(phenylene oxide) and polystyrene. High-resolution ^{13}C n.m.r. spectra of polymers can also be used for measuring microscopic chain dynamics. ^{13}C rotating-frame relaxation parameters observed for polycarbonate and poly(ethylene terephthalate) are related to the effects on motion of annealing, additives and structural substitutions. Individual relaxation rates are observed for individual carbons, so the behaviour of side groups is cleanly separated from that of the main chain. All of the line-narrowing and sensitivity-enhancing techniques applied to ^{13}C n.m.r. of solids work equally well for ^{15}N n.m.r. Use of ^{15}N rotating-frame and cross-polarization parameters leads to the assessment of the relative concentrations of ^{13}C–^{15}N and ^{12}C–^{15}N pair concentrations in the main chains of multiply labelled proteins. Such measurements can be used to characterize the rate of protein turnover in fully expanded soybean leaves, as well as the details of protein synthesis in cultured soybean cotyledons.

Introduction

Less than 10 years have passed since the sensitivity-enhanced cross-polarization n.m.r. experiment for natural-abundance ^{13}C in organic solids was introduced (Pines *et al.* 1973), and less than 5 years since this technique was combined with magic angle sample spinning to generate liquid-like high-resolution rare-spin n.m.r. spectra of solids (Garroway *et al.* 1976; Lippmaa *et al.* 1976; Schaefer & Stejskal 1976). Nevertheless, the combination experiment has gained a widespread popularity because of its inherent simplicity, and because of the ease of interpretation of the resulting spectra in terms of the structure and dynamics of typical organic solids.

In this paper, we shall illustrate the kinds of information currently being obtained by using cross-polarization magic angle spinning ^{13}C and ^{15}N n.m.r. We shall select examples from studies of generally complicated, usually intractable polymeric systems of practical importance.

Structural determinations with ^{13}C n.m.r.

(*a*) *Carbon-fibre precursors*

One route for production of a carbon fibre starts by a low-temperature pyrolysis in air of fibres made from polyacrylonitrile homopolymers or copolymers (figure 1*a*). Carbon fibres are

then produced by a subsequent high-temperature carbonization. Carbon fibres are used to make high-performance reinforced composite materials. While the characterization of the initial fibres and the intermediate partly aromatized, or oxidized, material is difficult by conventional spectroscopy, analysis by magic angle cross-polarization ^{13}C n.m.r. is straightforward.

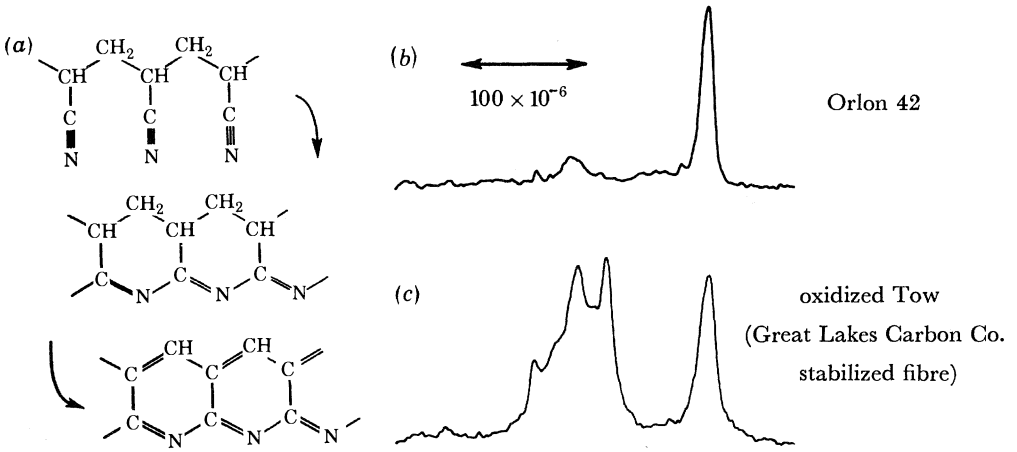

FIGURE 1. Cross-polarization 15.1 MHz ^{13}C n.m.r. spectra of chopped, predominantly polyacrylonitrile fibre (*b*) and of a low-temperature pyrolysed version of the same fibre (*c*) contained in a Beams–Andrew hollow rotor spinning at 2 kHz at the magic angle.

The spectrum of Orlon 42, which is predominantly polyacrylonitrile, consists of a high-field line arising from the aliphatic main-chain carbons, and a low-field line from the nitrile carbon (figure 1*b*). The latter is broadened by ^{13}C–^{14}N coupling not removed by magic angle spinning (Maricq & Waugh 1979). The extent to which the pyrolysed Orlon carbon-fibre precursor retains aliphatic character can be estimated by the relative intensity of the high-field line (figure 1*c*). With suitable model compounds, and with various fibre precursors pyrolysed to different degrees, some sense can also be made out of the observed four or five aromatic carbon lines. These assignments are ultimately important in understanding the carbonization process itself. (The effects of ^{14}N broadening can, however, be nasty. One way out of that dilemma is to perform single and double cross-polarization experiments on fibres made from ^{15}N-polyacrylonitrile, since 2 kHz spinning will completely remove ^{13}C–^{15}N dipolar broadening (Schaefer *et al.* 1979*a*).)

The 15.1 MHz ^{13}C n.m.r. spectra shown in figure 1 were each obtained from the time average of approximately 50 000 transients collected overnight, with magic angle spinning of the chopped fibres at 2 kHz in a 700 μl Beams–Andrew Kel-F hollow rotor, with matched spin-lock cross-polarization techniques with 2 ms single contacts and 40 kHz H_1's. Further details of the principles and execution of the combination magic angle cross-polarization experiment are presented in a preceding paper in this symposium by Professor Andrew.

The determination of the relative aliphatic character of the carbon-fibre precursor is, in principle, the same as determinations made of a variety of solid oil shales and coals (Vander-Hart & Retcofsky 1976; Bartuska *et al.* 1977; Resing *et al.* 1978; Miknis *et al.* 1979). In each instance, the determination is insensitive to most of the details of the magic angle cross-polarization procedures (within reasonable limits: spinning speed, contact time, r.f. field strengths, etc.), and interpretation of the results involves a simple measure of the ratios of

intensities of two lines in the spectra. The only real precaution that one need take is to avoid experiments on either highly paramagnetic or highly proton-deficient samples since, in either case, the reliability of the cross-polarization procedure to generate quantitatively representative carbon magnetizations for chemically different types of carbons becomes suspect (Taki *et al.* 1980).

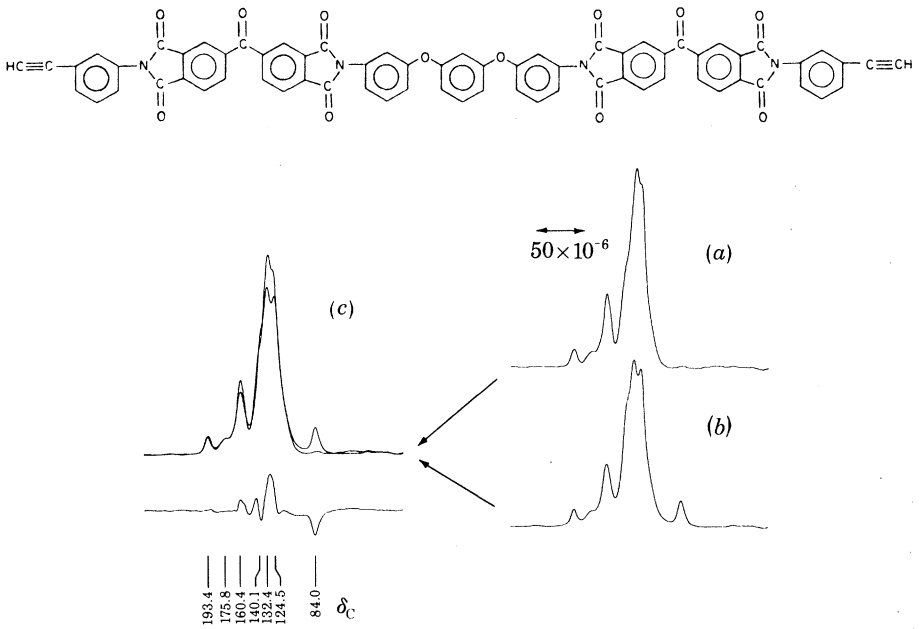

FIGURE 2. Difference spectrum (*c*) obtained by subtraction of a polyimide resin spectrum (with lines artifically broadened, (*b*)) from that of the cured polyimide polymer (*a*). Small deviations in the difference spectrum should be ignored since line broadening across the cured polymer spectrum may not be uniform.

(*b*) *Cross-linked resins*

Polyimide polymers have been developed over the last decade for applications as coatings, adhesives and thermosetting laminates where stability at temperatures up to 400 °C is required (Preston 1971). Although polyimides can be prepared by condensation polymerization of polyamic acids, such reactions liberate volatile by-products such as water during curing and consequently produce void-filled fabricated structures. The problem of void formation during curing and subsequent postcuring has been solved mainly with the use of acetylene-terminated polyimide pre-polymeric resins (figure 2, top) in which homopolymerization at elevated temperatures and pressures occurs without the formation of volatile byproducts (Bilow *et al.* 1975). Polyimide polymers formed in this fashion are void free and exhibit excellent thermal and physical properties. The mechanism of cure is believed to be aromatization of the acetylenic end groups but this has been impossible to verify owing to the intractability of the cross-linked resin.

The ^{13}C n.m.r. spectrum of the resin (figure 2*b*) has sufficient resolution for identification of peaks arising from the acetylenic carbons ($\delta_C = 84 \times 10^{-6}$), various aromatic carbons ($125–140 \times 10^{-6}$), the amide carbonyl and aryl carbons with oxygen substituents (160×10^{-6}), and the benzophenone carbonyls (193×10^{-6}). The resonance at $\delta_C = 176 \times 10^{-6}$ cannot be accounted for in the theoretical structure of the prepolymer, but its chemical shift and chemical history suggest its assignment to a carboxylic acid resulting from incomplete imidization of the prepolymer. Spectra of the insoluble cured polyimide (figure 2*a*) show changes in the line shape

of the aromatic carbon region and the diminution of intensity in the acetylenic carbon region. These changes are somewhat easier to see in a difference spectrum (figure 2*c*).

By using straightforward correlations between structure and isotropic carbon chemical shifts (Sefcik *et al.* 1979), it is possible to show conclusively that reactions involving the terminal acetylenic groups of the polyimide resin are, in fact, involved in the polymerization process, but that not more than 30% of these acetylenes can undergo cyclotrimerization or other condensation reactions. The remainder appear to be consumed by addition reactions. Furthermore, esterification can be eliminated as an additional cross-linking mechanism, and various constraints and limits on the degrees to which other chemical reactions occur can also be established. This is true even though the resolution of the spectra is limited to resonance bands (rather than resolved lines) so that only differences between spectra are easily interpreted.

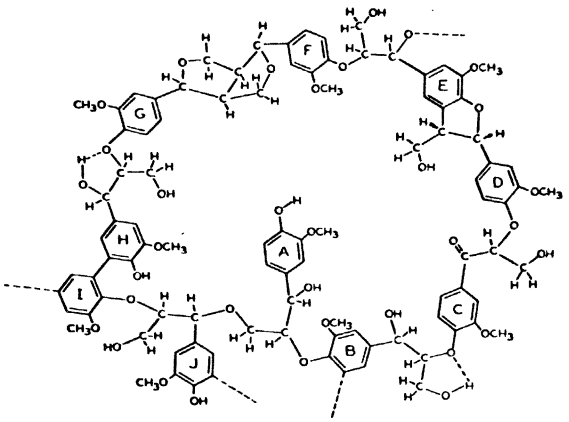

possible chemical structure for lignin

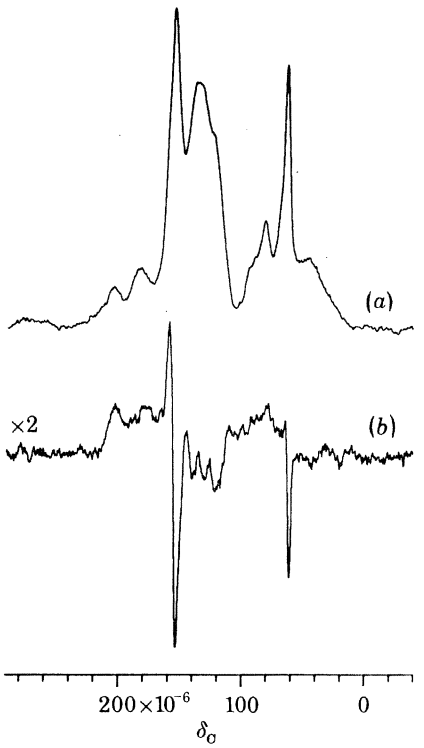

FIGURE 3. Magic angle cross-polarization ^{13}C n.m.r. spectrum of a lyophilized lignin (*a*) after 4 weeks of fermentation by a wood-rot fungus. In the difference spectrum (*b*), negative-going lines show the loss, and positive-going lines the gain, of carbons of a particular chemical shift due to metabolism between 1 and 4 weeks in the fermenter.

(*c*) *Solid metabolites of lignin fermentation*

Lignin is a major by-product of the paper industry. A possible use for lignin is as an extender for plastics. If lignin could be chemically modified to react with, for example, polyesters, an inexpensive cross-linked copolymeric mix might be a useful product.

Magic angle cross-polarization ^{13}C n.m.r. can be used to characterize the extent to which *Coriolus versicolor* (a wood-rot fungus) generates insoluble metabolic products starting with a lignin slurry as a carbon source (Schaefer *et al.* 1980*a*). Solid samples were removed from a fermenter over an 8 week period, washed, lyophilized, and examined by n.m.r. After 1 week in the fermenter

almost nothing had happened to the lignin. Fermentation is slow because the lignin is not an optimal solid state carbon source. A small amount of cellulose added to the fermenter along with the lignin was consumed during this period. Substantial changes in the lignin occurred between 1 and 4 weeks, including the generation of vinyl aldehyde linkages. These were identified with the positive-going line near $\delta_C = 200 \times 10^{-6}$ in the lignin difference spectrum (figure 3, bottom). Just as in figure 2, the negative-going lines indicate the disappearance of carbons of a particular type.

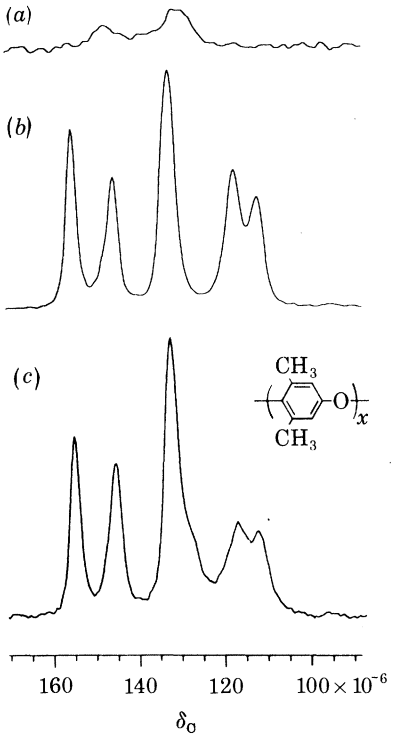

FIGURE 4. Magic angle cross-polarization ^{13}C n.m.r. spectra of the aromatic carbon regions of (*a*) d_8-polystyrene, (*b*) poly(phenylene oxide) homopolymer, and (*c*) a 25:75 blend of the two polymers.

The change in lignin between 4 and 8 weeks fermentation is measurable but not dramatic. We suspect that the fungus has settled down to a steady-state programme of reducing lignin to soluble products rather than activating a variety of enzymes that only slightly chemically alter lignin, thus leaving behind an insoluble product. In any event, after 8 weeks, about 9% of all the carbons of lignin are present in solid metabolites chemically different from the starting material, and about 10% of these altered carbons are now in a functionality that can be exploited as an industrial chemical intermediate.

(*d*) *Polymeric blends*

In the previous three examples, cross-polarization ^{13}C n.m.r. determinations of molecular structure were performed on heterogeneous *solid* samples simply because there was little other choice. That is, carbon fibre precursors, cross-linked resins and solid lignin metabolites are non-crystalline, insoluble materials not amenable to conventional chemical or spectroscopic analysis.

However, there are structural problems where it is precisely the structure of the solid itself that is of interest. For example, poly(2,6-dimethylphenylene oxide) (PPO) forms a nominally

homogeneous blend, or solid solution, with polystyrene (PS). These blends are, more accurately, homogeneous on about a 10 nm scale, as established by low-angle neutron scattering experiments (Wignall *et al.* 1980). The question arises as to whether PPO–PS blends are also homogeneous on the much smaller scale established by short-range n.m.r. chemical-shift and spin–lattice parameters.

The protonated aromatic carbon doublet of PPO ($\delta_C = 115 \times 10^{-6}$) is broadened and considerably more complex in a 25:75 blend than in the homopolymer (figure 4). This observation is, in fact, easier to make on a blend with d_8-PS, which avoids the strong aromatic PS resonance at $\delta_C = 125 \times 10^{-6}$. (Interchain carbon–deuterium dipolar interactions can be neglected.) In amorphous materials, ^{13}C isotropic chemical shifts arise from shielding effects that extend no more than, say, 1 nm (Tonelli 1979). The fact that changes in isotropic shifts (or line-shapes) of the blend (relative to the component homopolymer) can be observed means that mixing in PPO–PS blends is indeed on an individual chain-for-chain basis. These shifts may be induced either by direct interchain shielding, or by indirect conformationally induced effects. In either event, the interacting chains must be nearest neighbours.

The evidence from the ^{13}C chemical shifts shows that the PPO–PS blends are intimately mixed but does not show that they are uniformly mixed. The latter information is, however, available from rotating-frame *proton* spin-lattice relaxation times (Schaefer *et al.* 1979*b*). The high-resolution magic angle techniques used to obtain ^{13}C n.m.r. spectra in solids can be employed to measure individual $T_{1\rho}$'s for protons attached to different kinds of carbons. This is possible because the final evolution of the carbon signal in a cross-polarization experiment tracks the $T_{1\rho}$ decay of the protons. Under high-resolution conditions, individual carbon resonances follow the protons to which they are most closely coupled and thus are capable of resolving $T_{1\rho}(H)$ differences between protons that might be difficult to detect if the $T_{1\rho}(H)$ process were obtained directly from the composite proton signal (McCall 1971). Owing to spin diffusion, proton $T_{1\rho}$'s of a multi-component or multi-phase system are strongly dependent on spatial proximity, and hence on uniformity of mixing of the various components.

For a matched spin-lock cross-polarization transfer, the carbon magnetization, S, is given by (Stejskal *et al.* 1979):

$$\frac{dS}{dt} = \frac{S_0 e^{-t/T_{1\rho}(H)} - S}{T_{IS}} - \frac{S}{T'_{\rho L}},$$

where S_0 is the maximum carbon polarization available in a matched spin-lock experiment with no dissipative processes; $T_{1\rho}(H)$ is the proton rotating-frame spin–lattice relaxation time constant; T_{IS} is the proton–carbon matched spin-lock cross-polarization time constant; and $T'_{\rho L}$ is the carbon rotating-frame spin–lattice relaxation time constant in the presence of dipolar decoupling of the protons.

Thus,

$$S = (S_0/T_{IS}) \frac{e^{-t/T_{1\rho}(H)} - e^{-t(1/T_{IS}+1/T'_{\rho L})}}{1/T_{IS} + 1/T'_{\rho L} - 1/T_{1\rho}(H)},$$

and since $T'_{\rho L} \gg T_{IS}$ we can make the approximation

$$S \approx (S_0/T_{IS}) \frac{e^{-t/T_{1\rho}(H)} - e^{-t/T_{IS}}}{1/T_{IS} - 1/T_{1\rho}(H)}.$$

In addition, since $T_{1\rho}(H) \gg T_{IS}$, when $t \gg T_{IS}$,

$$S \approx S_0 e^{-t/T_{1\rho}(H)}.$$

Thus, from a semilogarithmic plot of S against t, we obtain $T_{1\rho}(H)$.

Figure 5 displays $T_{1\rho}(H)$ relaxation as detected by the protonated, main-chain carbons of PPO, high molecular mass atactic PS, isotactic PS(i-PS) and three PPO–PS (75:25) blends. The protons were spin-locked in a field of 37 kHz. The initial proton–carbon cross-polarization transfer was complete within several hundred microseconds so that the first points shown (at 2 ms) are fully indicative of the $T_{1\rho}(H)$ process. It can be observed in the blends that the PPO and PS carbons detect slightly different $T_{1\rho}(H)$ processes, and, more importantly, that the PS decays are clearly not first order.

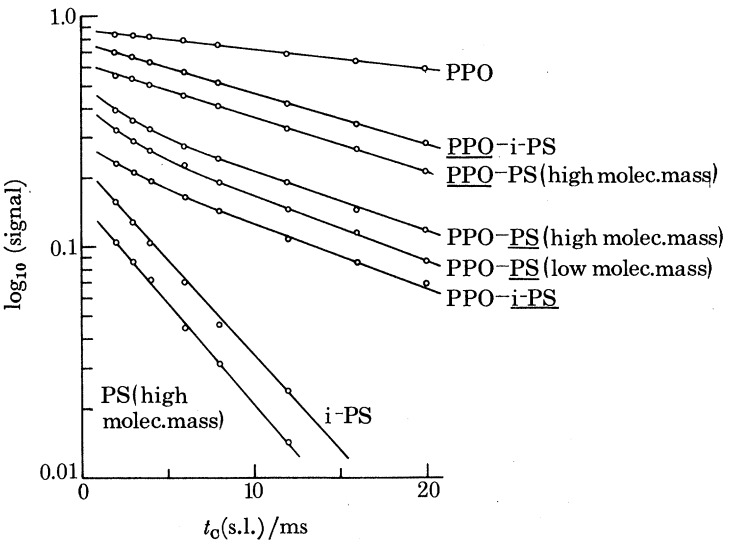

FIGURE 5. Plots of carbon magnetization generated by long-term matched spin-lock cross-polarization transfers yielding $T_{1\rho}$'s for protons attached to main-chain carbons of PPO, PS and a variety of 75:25 PPO–PS blends under magic angle spinning.

Part (perhaps 5–10 %) of the initial decay of the PS protons can be attributed to small regions where the PS is not fully dispersed and mixed with PPO and hence relaxes more like PS homopolymer (Schaefer *et al.* 1979*b*). The net result is an effective phase separation and a distribution of PS relaxation rates. This distribution cannot be explained in terms of local statistical fluctuations of homogeneous mixing, since random mixing of PS with proton-deficient perdeutero-polystyrene results in just a single, average, increased $T_{1\rho}(H)$. With an assumption of phase separation for a part of the PPO–PS blend, the relaxation behaviour of the remaining part is virtually indistinguishable from that of the PPO–i-PS blend. These regions of poorly dispersed PS need not be more than places where awkwardly kinked atactic PS tends to fold back on itself, or where a few independent chains have aggregated. The resulting regions must be in relatively poor contact with nearby PPO chains so that an effective phase separation can occur. The extent of this phase separation could well depend on temperature-dependent subtleties of moulding and quenching during processing.

Isotactic PS, being more regular than atactic polystyrene, is perhaps less likely to aggregate, or phase separate, on mixing with PPO. Nevertheless, the possibility cannot be ruled out that some or all of the minor curvature in the i-PS relaxation curve is due to such regions. However, it is *not* necessary to postulate such regions to fit the PPO–i-PS data because simple models of homonuclear cross relaxation between chemically different, uniformly mixed protons of PPO and

i-PS can be used to fit the shape of the relaxation curves reasonably well. These same models fail to explain the more pronounced curvature in the PPO–PS blends, so that an explanation of the more pronounced curvature in terms of incomplete cross relaxation in a homogeneously mixed blend of PPO and atactic PS is not possible. We plan to report further details of these calculations later.

Polymer chain dynamics with ^{13}C n.m.r.

(*a*) *Molecular motion and* $T_{1\rho}$(C)

^{13}C spin-lattice parameters are free from averaging arising from spin diffusion, at least for most natural-abundance experiments, and so are potentially useful. In fact, the ^{13}C rotating-frame spin–lattice relaxation time, $T_{1\rho}$(C) (see below), has been shown qualitatively to characterize the room-temperature mid-kilohertz main-chain motions of glassy polymers, and has been empirically linked to the mechanical properties of the polymers, which presumably depend on this motion (Schaefer *et al.* 1977). Such a connection is possible because (1) both n.m.r. and mechanical measurements can be made on the same sample under end-use conditions, (2) the high resolution of the ^{13}C n.m.r. experiment permits an unambiguous separation of important main-chain motions from unimportant side-chain motions, and (3) the mechanically important low- to mid-kilohertz frequency range can be probed conveniently in the $T_{1\rho}$(C) experiment by variation of H_1(C) rather than by variation of temperature. The latter advantage eliminates the need for temperature–frequency superposition principles of questionable validity.

There is, however, a complication in the use of ^{13}C $T_{1\rho}$'s. The possibility exists (Schaefer *et al.* 1977) of static ^{1}H-^{13}C spin–spin interactions shortening $T_{1\rho}$ and so confusing its interpretation as a motional parameter. A quantitative description of $T_{1\rho}$(C) of protonated main-chain carbons involves an estimate of the competition between two relaxation pathways. For carbons in rigid polymers having tightly coupled protons, a likely relaxation mechanism is by a spin–spin interaction. Strong, static ^{1}H–^{1}H interactions give rise to proton spin flips and a broad dipolar fluctuation spectrum having substantial spectral density at the ^{13}C rotating-frame Larmor frequency. Consequently, mutual spin flips can occur from spin-locked carbons to protons, resulting in a spin–spin polarization transfer which dominates $T_{1\rho}$(C). Polymers for which this is known to occur at room temperature include crystalline polyoxymethylene (Stejskal *et al.* 1979), crystalline polyethylene (VanderHart & Garroway 1979), and crystalline poly(ethylene terephthalate) (Sefcik *et al.* 1980).

For carbons in glassy polymers in which strong ^{1}H-^{1}H static dipolar interactions are absent because of molecular motion or large inter-proton distances, or some combination of these, a completely different situation can exist. The proton dipolar fluctuation spectrum now has little density at the carbon Larmor frequency for typical H_1(C)'s of 30 kHz or more. Instead, spectral density generated by fluctuating dipolar fields associated with rotations of ^{13}C–^{1}H internuclear vectors can be effective in producing ^{13}C spin flips. In other words, the dominant mechanism for $T_{1\rho}$(C) relaxation is now spin-lattice in character.

(*b*) *Comparison of* $T_{1\rho}$(C) *and* T_{IS} (a.d.r.f.)

The most direct and quantitative measure of the relative importance of spin–spin and spin–lattice contributions to $T_{1\rho}$(C) is by a comparison of the *average* steady-state values of polarization transfers observed in $T_{1\rho}$(C) and T_{IS} (a.d.r.f.) experiments (Stejskal *et al.* 1979). In the

first experiment, after a matched, spin-lock Hartman–Hahn generation of a carbon polarization, the proton r.f. field is turned off abruptly. After about a 50 μs delay, measurement of the initial steady-state rate of decay of the total carbon magnetization held in its rotating field yields $\langle T_{1\rho}(\mathrm{C})\rangle$, the average carbon spin-lock lifetime.

In the second experiment, after a spin locking of the protons, the ^{1}H r.f. field is turned off in times of about 0.5 ms (long compared with proton T_2's), so that the order established by the spin lock is transferred to the local dipolar field. This process is called an adiabatic demagnetization in the rotating frame (a.d.r.f.). Order in the dipolar field can be maintained in a *non-spinning* sample for a characteristic time, $T_{1\mathrm{D}}$. At $t = 0$ (defined as 50 μs after the turning on of a carbon r.f. field), an estimate of the initial rate of *non-transient* polarization transfer from the local field to the ^{13}C r.f. field yields $(\mathrm{d}S/\mathrm{d}t)_{t=0}$ where (Stejskal *et al.* 1979)

$$(\mathrm{d}S/\mathrm{d}t)_{t=0} = S_0/\langle T_{IS}(\text{a.d.r.f.})\rangle - S_i/\langle T_{1\rho}(\mathrm{C})\rangle;$$

S_i is the transient carbon polarization developed in the 50 μs immediately after the turning on of the carbon r.f. field, and $S_0 \approx \mathrm{S_m}\,(\gamma_S H_1(\mathrm{C})/\gamma_I H_{\mathrm{L}})\,\epsilon$. In the above relation, γ_S and γ_I are the gyromagnetic ratios of S and I spins, respectively, and S_0 is the total carbon polarization available in an experiment with no dissipative relaxation processes. The latter is evaluated from, first, S_{m} the matched spin-lock carbon polarization; secondly, H_{L} (equal to $\sqrt{(\frac{1}{3}M_2^{\mathrm{II}})}$, where M_2^{II} is the proton second moment obtained from T_2(H) in either direct proton n.m.r. experiments or in ^{13}C separated local field experiments (Schaefer *et al.* 1980*b*)); and, thirdly, ϵ the average net efficiency of the proton a.d.r.f. process (a constant, generally between 0.50 and 0.75).

The rate of relaxation represented by $\langle T_{1\rho}(\mathrm{C})\rangle^{-1}$ is the sum of a spin–lattice relaxation component and a spin–spin component, the latter given by $\langle T_{IS}(\text{a.d.r.f.})\rangle^{-1}$. If there is no spin–lattice contribution, $T_{1\rho}(\mathrm{C})$ equals T_{IS}(a.d.r.f.). Thus, a simple ratio of $\langle T_{1\rho}(\mathrm{C})\rangle$: $\langle T_{IS}(\text{a.d.r.f.})\rangle$ determines the relative importance of spin–spin and spin–lattice contributions to $\langle T_{1\rho}(\mathrm{C})\rangle$. If the ratio is close to zero, $\langle T_{1\rho}(\mathrm{C})\rangle$ is determined by motional processes; if the ratio is close to one, $\langle T_{1\rho}(\mathrm{C})\rangle$ is spin–spin in origin.

For example, the spin–spin contribution to $\langle T_{1\rho}(\mathrm{C})\rangle$ for quenched (glassy) poly(ethylene terephthalate) is no more than a small percentage since the observed ratio is less than 0.1 for $H_1(\mathrm{C}) = 37$ kHz (Sefcik *et al.* 1980). The ratio is even smaller for polycarbonate; that is, $\langle T_{1\rho}(\mathrm{C})\rangle$ is much smaller than $\langle T_{IS}(\text{a.d.r.f.})\rangle$ for these H_1's. In fact, a typical spin–spin $\langle T_{IS}(\text{a.d.r.f.})\rangle$ increases by about a factor of 10 for each increase in $H_1(\mathrm{C})$ equal to half of the proton line width (Demco *et al.* 1975). For polycarbonate the full proton line width is about 20 kHz, so if $\langle T_{1\rho}(\mathrm{C})\rangle$ were equal to $\langle T_{IS}(\text{a.d.r.f.})\rangle$, $\langle T_{1\rho}(\mathrm{C})\rangle$ would increase by about 10^4 for an increase of $H_1(\mathrm{C})$ from 20 to 60 kHz. The observed increase is less than a factor of 2 (Steger *et al.* 1980).

(*c*) $T_{1\rho}(\mathrm{C})$ *in polycarbonate and poly(ethylene terephthalate)*

Based on the above discussion, it is clear that the observed protonated aromatic carbon $T_{1\rho}$ relaxation characterizes mid-kilohertz main-chain motions in both poly(ethylene terephthalate) (PET) and polycarbonate. Typical $T_{1\rho}(\mathrm{C})$ results for polycarbonate are shown in figure 6. The spectrum of polycarbonate consists of five lines. These have been identified (Schaefer *et al.* 1977) from left to right, in order of increasing magnetic field, as a combination line arising from the carboxyl and non-protonated aromatic carbons, two lines due to the protonated aromatic carbons, the aliphatic quaternary carbon line, and the methyl carbon line, respectively. The

PHILOSOPHICAL TRANSACTIONS OF THE ROYAL SOCIETY A MATHEMATICAL, PHYSICAL & ENGINEERING SCIENCES

component of each of these lines which relaxes first in a $T_{1\rho}(C)$ experiment appears motionally broadened (figure 6, difference spectra), even in experiments with H_1's as large as 60 kHz (Steger *et al.* 1980).

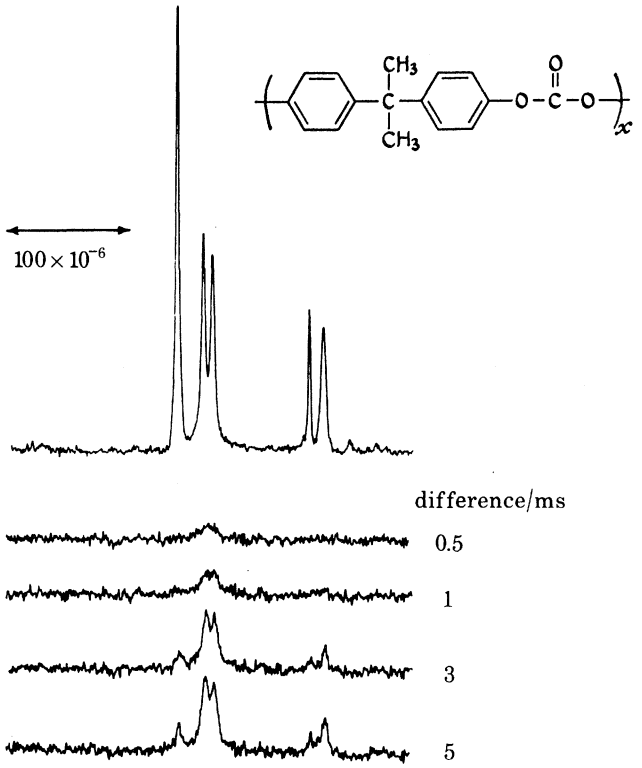

FIGURE 6. Magic angle cross-polarization ^{13}C n.m.r. spectra of a quenched polycarbonate in a $T_{1\rho}(C)$ experiment with $H_1(C) = 28$ kHz. The top spectrum was obtained by using a carbon rotating-frame time of 0.05 ms after removal of the proton r.f. field. The bottom four spectra are differences between the top spectrum and the spectra obtained for correspondingly longer spin-lock times in the carbon rotating frame.

Such motions presumably involve cooperative torsional oscillations of phenyl groups within conformations locked into the glass by interchain steric interactions. These motions must involve angular excursions of more than 10° (Cheung & Yaris 1980) and are represented by a broad distribution of correlation frequencies of up to 10^5 Hz (or higher) at room temperature. The motions (as monitored by $T_{1\rho}(C)$) are severely restricted by some structural modifications (introducing chlorine substituents around the flexible carbonate group, for example, or replacing the symmetrical *para-para* phenyl substitution by an asymmetrical *ortho-para* linkage), but are not restricted by the presence of various anti-plasticizing chemical additives (Steger *et al.* 1980).

Just as with polycarbonate, quenched PET is a highly ductile material. This ductile behaviour appears to arise from cooperative high-frequency components of motion associated with trapped, non-equilibrium ethylene configurations. These motions are the precursors to plastic flow. Annealing removes these motions, resulting in either slow cooperative ethylene- and phenyl-group motions, or fast but localized (independent, non-cooperative) phenyl-group motions, neither of which is well suited to initiating plastic flow. Loss of just a few high-frequency cooperative motions is apparently sufficient to precipitate a change in failure mode from ductile to brittle (Sefcik *et al.* 1980). Consistent with this notion, motionally dominated ethylene carbon

$\langle T_{1\rho}(\mathrm{C})\rangle$'s of PET increase significantly when quenched films are annealed at 61 °C (figure 7). All the spin–spin parameters for these quenched and annealed PETs are almost identical. Naturally, this kind of direct connection between microscopic chain dynamics and macroscopic physical properties is of considerable diagnostic value in understanding the mechanical behaviour of a commercial polymer that has undergone complicated processing into a final product.

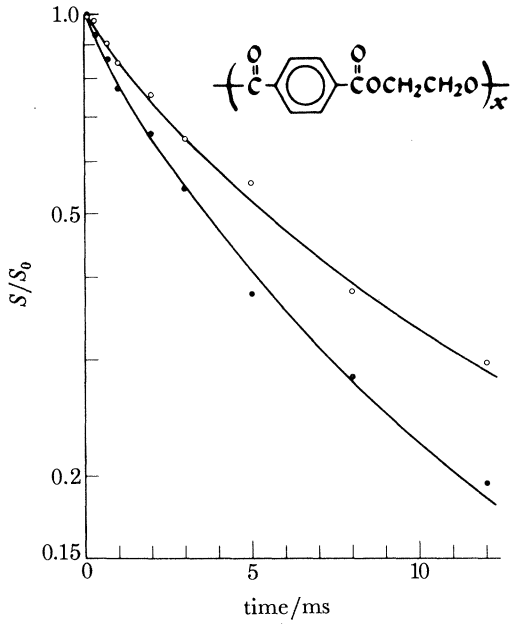

FIGURE 7. ^{13}C 37 kHz magic angle rotating-frame relaxation data for the methylene carbons of poly(ethylene terephthalate) showing the dispersion that results from a distribution of relaxation times. The average relaxation time, represented by the initial slope of the relaxation curve, is 3.5 ms for the quenched polymer (filled circles) and 6.0 ms for the annealed polymer (open circles). The annealing was performed at 61 °C for 350 h.

NITROGEN METABOLISM WITH ^{15}N N.M.R.

(*a*) *Resolution of* ^{15}N *n.m.r. spectra of uniformly labelled proteins*

The absence of a relatively long-lived radioisotope of nitrogen has limited research of the transport and metabolism of nitrogen in plants. The 10 min half life of ^{13}N prohibits experiments lasting much more than 2 h (Wolk *et al.* 1976). During this time, the radioisotope label must be prepared, administered, extracted and counted (Meeks *et al.* 1978). Characterization of the details of complicated protein synthesis by this procedure appears difficult. Stable-isotope ^{15}N labelling experiments have been performed in the past with nitrogen-containing parts of the plant degraded, extracted, chromatographically separated, and the label detected by atomic emission spectroscopy (Lewis & Pate 1973) or reduced to N_2 and detected by mass spectrometry (Bauer *et al.* 1977). These destructive analyses run the risk of chemically altering the sample (losing information about amide nitrogen, for example) and depend on the efficacy of an established chromatographic procedure. Clearly, detection of ^{15}N labels with the techniques developed for high-resolution ^{13}C n.m.r. of intact solids should avoid many of the problems afflicting earlier nitrogen metabolism experiments.

The resolution achieved by magic angle ^{15}N n.m.r. is sufficient to permit a determination of the relative concentrations of amide and amine nitrogens in the seed and pod of a soybean plant

at various stages of development (Schaefer *et al.* 1979*c*). In addition, a few chemically different amine nitrogens can be identified. For example, the low-field side of the intense protein main-chain amide nitrogen line of the spectrum (figure 9*a*) of a mature seed from a soybean plant grown on ^{15}N-enriched fertilizer can be assigned to histidine ring nitrogens (Wüthrich 1976), while the high-field side can be assigned, for the most part, to the NH_2 nitrogens of arginine residues (Wüthrich 1976). The high-field amine nitrogen resonance observed in the spectrum of the immature pod (figure 8*b*) is probably due to high concentrations of free amino acids, presumably the transport species glutamine.

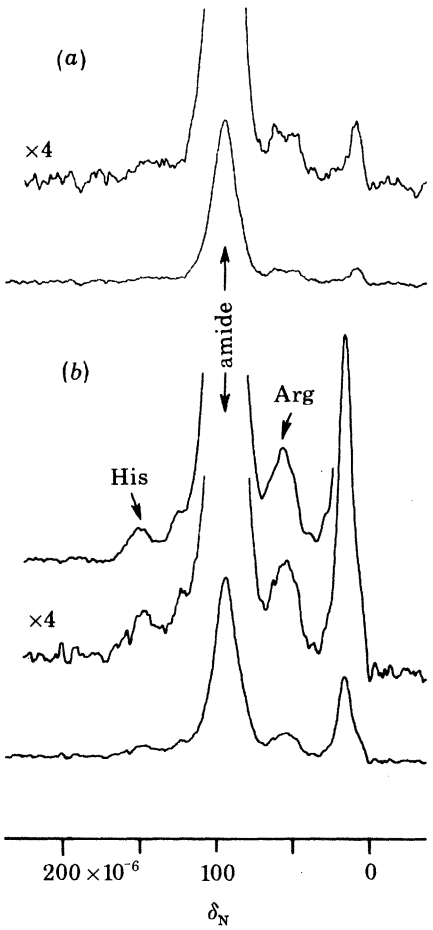

FIGURE 8. Cross-polarization 9.12 MHz ^{15}N n.m.r. spectra of various parts of a uniformly labelled ^{15}N soybean plant removed at different points of development. The spectra were obtained with magic angle spinning at 1.7 kHz. The shift, δ_N, is measured from solid ammonium sulphate. For the upper spectrum in (*b*), eight times as many scans were taken.

Although not appearing in figure 8, the ^{15}N resonances from proline, alanine, NO_3^- and NH_4^+ are also well resolved. Thus the magic angle cross-polarization ^{15}N n.m.r. experiment offers a simple and discriminating way to monitor total nitrogen flux and incorporation during complicated metabolism. This is particularly useful both in studies with whole plants and non-specific labels, as well as in studies involving plant cells and organs maintained in culture on specifically labelled nutrients.

(b) Chemical-bond labelling and double-cross polarization n.m.r.

In fact, one of the most powerful applications of stable-isotope labelling is in the use of double labels (Schaefer *et al.* 1980*c*) in cell and organ cultures. For example, a culture medium containing two amino acids as nutrients, one labelled with ^{15}N and the other with ^{13}C, can be used to grow soybean cotyledons. The resulting protein synthesized by the cotyledon can then be examined *in situ* by both ^{15}N and ^{13}C n.m.r. In addition, the presence of ^{15}N–^{13}C labelled bonds can be determined in the solid state by *double-cross polarization* n.m.r. thereby revealing highly specific details of protein metabolism.

Double-cross polarization (d.c.p.) is a serial extension of cross polarization (c.p.) to three-spin systems (^{1}H, ^{13}C and ^{15}N). The experiment involves first a transfer of polarization from protons to either carbons or nitrogens, followed by a turning off of the proton channel together with a matched spin-lock contact of carbons and nitrogens. Either ^{13}C or ^{15}N spins can then be observed resulting in d.c.p. spectra, which contain information about nitrogen–carbon coupling

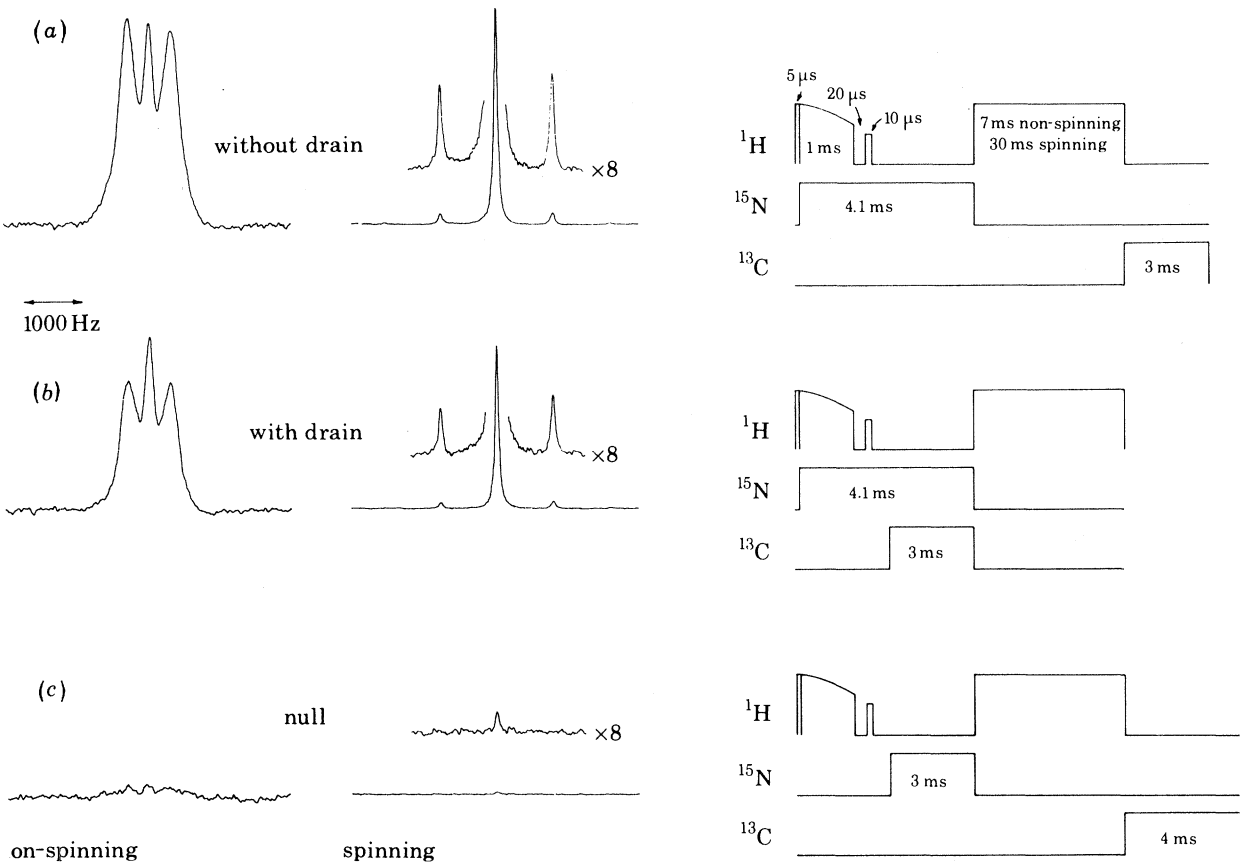

FIGURE 9. Single (*a*) and double (*b*) cross-polarization ^{15}N n.m.r. spectra of 25% $^{15}NH_2{}^{13}CH_2COOH$ (99% ^{15}N; 90% ^{13}C) recrystallized with 75% natural-abundance glycine with (middle) and without (left) magic angle spinning at 1.0 kHz. Pulse sequences employed are shown at the right. The double cross-polarization procedure involved a depletion of ^{15}N polarization (transferred from protons initially spin-locked at 50 kHz) by a Hartmann–Hahn contact with carbons at 25 kHz. The ^{13}C r.f. was phase modulated to prevent an accumulation of carbon polarization. The decrease of ^{15}N polarization arising from nitrogens coupled to carbons can be seen either in the decrease of the doublet:singlet ratio of the non-spinning spectra or in the decrease of the sideband:centreband ratio of the spinning spectra. Direct transfer of polarization from protons to nitrogens under mismatched conditions is negligible (*c*). Extraneous carbon pulses were included in the single cross-polarization experiments to ensure equivalent r.f. heating effects.

with sensitivity greater than that achieved by c.p. n.m.r. between nuclei with small γ and long T_1 nuclei (Schaefer *et al.* 1979*d*). D.c.p. n.m.r. can be performed by using either a two-coil system, one coil of which is doubly tuned, or by triply tuning a single coil. By using 300 kW transmitters for each of the ^{15}N and ^{13}C channels, and a 200 W transmitter for the ^{1}H channel, typical H_1's of 25, 40 and 50 kHz, at 9.12, 22.6 and 90 MHz respectively, can be achieved in an 11 mm diameter coil. Thus, matched spin-lock transfers between all three nuclei can be made at 25 kHz.

A more effective use of the available H_1's is possible if the protons are spin locked by using the 50 kHz H_1 which is then adiabatically reduced to 25 kHz, permitting a matched c.p. transfer to nitrogens. Under these conditions, the normal c.p. ^{15}N spectrum of isolated double-labelled glycine (99% ^{15}N; 90% ^{13}C) consists of a doublet and a singlet (figure 9*a*). The former is due to ^{15}N–^{13}C pairs and the latter to ^{15}N–^{12}C pairs. The integrated intensity of the ^{15}N–^{12}C singlet is close to 10% of the entire spectrum. A d.c.p. experiment can now be performed by turning off the proton H_1 and matching nitrogen and carbon H_1's. Polarization is drained from the ^{15}N spin system by coupling to directly bonded ^{13}C spins, thereby diminishing the intensity of the doublet (figure 9*b*, left). The single pulse following turn-off of the proton H_1 helps to eliminate any dipolar order in the ^{1}H local field (for a non-spinning sample) and hence the possibility of a significant direct transfer (VanderHart & Garroway 1979) from protons to nitrogens (figure 9*c*). The version of the d.c.p. experiment involving a drain of polarization and subsequent detection of the depleted rare spin can also be performed with magic angle spinning (figure 9*b*, middle). Since modulation effects due to spinning (Stejskal *et al.* 1977) are similar for carbons and nitrogens, the ^{13}C–^{15}N Hartmann–Hahn match is unchanged by high-speed sample rotation.

A ^{15}N d.c.p. spectrum can be used to measure the relative concentrations of ^{15}N–^{13}C and ^{15}N–^{12}C pairs in a partly double-labelled solid. This can be achieved despite the elimination of ^{15}N–^{13}C dipolar splittings by magic angle spinning. By determining the ^{15}N $T_{1\rho}$ relaxation times with ($T_{1\rho}$(NC)) and without ($T_{1\rho}$(N)) matched nitrogen–carbon contacts, the relative concentration of ^{15}N–^{13}C pairs can be determined by using the relation $1/\langle T_{1\rho}(\mathrm{NC})\rangle = f/\langle T_{\mathrm{NC}}(\mathrm{s.l.})\rangle + 1/\langle T_{1\rho}(\mathrm{N})\rangle$, where the brackets indicate an average value and f is the fraction of labelled pairs. Values for nitrogen–carbon matched spin-lock transfer times, T_{NC}(s.l.), for various types of carbon–nitrogen covalent bonds can be determined in separate experiments. The $T_{1\rho}$'s are determined by experiments similar to those illustrated in figure 9, and discussed earlier in this paper in the section dealing with polymer chain dynamics and $T_{1\rho}$(C).

(*c*) *Protein turnover in soybean leaves*

During senescence, the protein in soybean leaves degrades and is transported to the maturing ovules, or seeds, where it is transformed into storage protein (Huffaker & Peterson 1974). Thus, a natural mechanism is in place in soybean leaves for protein degradation. A question arises as to whether before senescence, a mature, fully expanded leaf having a fixed concentration of protein (mostly ribulose bisphosphate carboxylase, the CO_2-fixing enzyme) undergoes rapid protein turnover, so that the steady-state carboxylase content of the mature leaf is, in fact, the result of a dynamic balance between continuous rapid protein synthesis and degradation.

The answer to this question can be obtained by using ^{13}C and ^{15}N double labelling, together with d.c.p. n.m.r. (Skokut *et al.* 1979). Fully expanded leaves of soybean plants (*Glycine max* L. cv. Elf) 6 weeks old, grown on $^{15}NH_4$ $^{15}NO_3$, were exposed to 90% $^{13}CO_2$ (325/10^6, 21% O_2) for 1–7 days and then returned to normal conditions over a 40 day period after the exposure to

PHILOSOPHICAL TRANSACTIONS OF THE ROYAL SOCIETY A MATHEMATICAL, PHYSICAL & ENGINEERING SCIENCES

^{13}C label. ^{15}N d.c.p. spectra were obtained from each lyophilized leaf and were used to determine the percentage of ^{15}N–^{13}C pairs in the peptide backbone. The latter will be high if protein turnover in the leaves was fast during the labelling period and if the leaf was harvested soon after the completion of the $^{13}CO_2$ labelling. A measure of the rate of protein turnover can be made both from the rate of incorporation of ^{13}C into peptide linkages (as determined by d.c.p.), as well as by comparison of its disappearance from comparable labelled leaves harvested at different times from different plants after their return to a natural abundance atmosphere. These measures are not confused by the kinetics of incorporation of label into side chains.

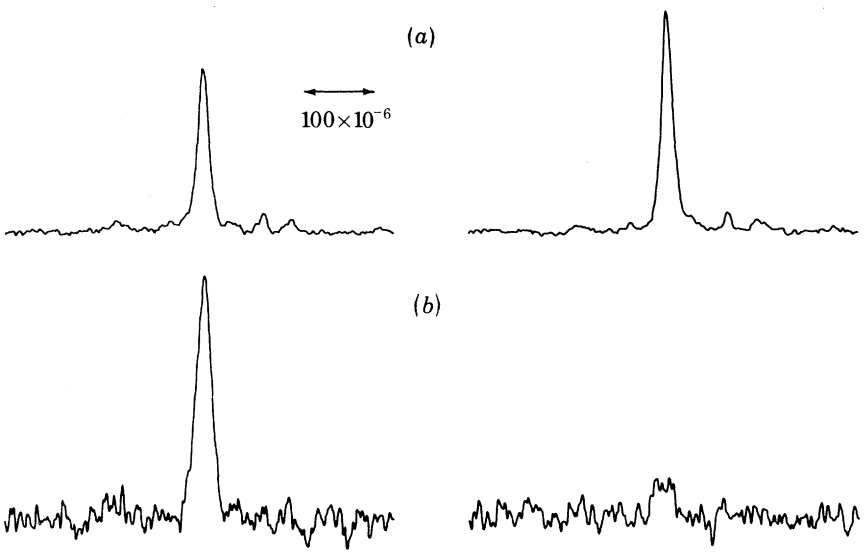

FIGURE 10. Magic angle cross-polarization ^{15}N n.m.r. spectra of ^{15}N-enriched lyophilized soybean leaves exposed to $^{13}CO_2$ (left) and $^{12}CO_2$ (right) during active photosynthesis. (*a*) Spectra obtained with the pulse sequences of figure 9*b* with a nitrogen spin lock of 7 ms and the carbon r.f. off resonance by 60 kHz; 2000 scans. (*b*) Spectra from double cross-polarization 7 ms direct-difference experiments in which the carbon r.f. is first off resonance and then on resonance; 60000 scans. The positive signal that accumulates is a measure of the concentration of ^{15}N–^{13}C pairs in the labelled leaf protein.

Typical ^{15}N n.m.r. spectra of labelled leaves are shown in figure 10. The relatively fast, rotating-frame relaxation rates of the histidine, arginine and lysine nitrogen lines (at 25 kHz) means that ^{15}N n.m.r. spectra are dominated by the main-chain amide line after a 7 ms nitrogen spin lock (figure 10*a*). The direct difference spectra (figure 10*b*) were obtained by using the pulse sequence shown in figure 9*b* twice. First, a positive signal was generated with the ^{13}C r.f. shifted off resonance by 60 kHz (so that no ^{15}N–^{13}C drain occurred), and then a second signal was generated with the same pulse sequence but with the ^{13}C r.f. on resonance. This second signal was subtracted from the first signal so that only the direct difference accumulated. The ratios of the difference signals to the drain-free signals (as a function of spin-lock time) ultimately yield the $T_{1\rho}$'s and hence the ^{15}N–^{13}C concentrations. For the two leaves of figure 10 this translates into a ^{13}C peptide linkage concentration of 23.2% for the labelled leaf, and 1.2% for natural abundance carbon leaf. (The labelled leaf was rapidly growing during its 7 day labelling period and so incorporated a considerable amount of ^{13}C into protein.) Similar experiments on about 50 labelled leaves have shown that the protein turnover time constant for *mature* soybean leaves is about 30 days. That is, before senescence, leaf protein in general, and carboxylase in particular, are highly stable.

References (Schaefer *et al.*)

Bartuska, V. J., Maciel, G. E., Schaefer, J. & Stejskal, E. O. 1977 *Fuel* **56**, 354–358.
Bauer, A., Urquhart, A. A. & Jay, K. W. 1977 *Pl. Physiol.* **59**, 915–919.
Bilow, N., Landis, A. L. & Milles, L. J. 1975 U.S. Patent no. 3 879 349.
Cheung, T. T. P. & Yaris, R. 1980 *J. chem. Phys.* **72**, 3604–3616.
Demco, D. E., Tegenfeldt, J. & Waugh, J. S. 1975 *Phys. Rev.* B **11**, 4133–4151.
Garroway, A. N., Moniz, W. B. & Resing, H. A. 1976 *Prepr. Div. Org. Coatings Plastics Chem.* **36**, 133–138.
Huffaker, R. C. & Peterson, L. W. 1974 *A. Rev. Pl. Physiol.* **25**, 363–392.
Lewis, O. A. M. & Pate, J. S. 1973 *J. exp. Bot.* **24**, 596–606.
Lippmaa, E., Alla, M. & Tuherm, T. 1976 *Proc. XIX Congress Ampere* (ed. H. Brunner, K. H. Hausser & D. Schweitzer), pp. 113–118. Heidelberg: Group Ampere.
McCall, D. W. 1971 *Acct. chem. Res.* **4**, 223–232.
Maricq, M. M. & Waugh, J. S. 1979 *J. chem. Phys.* **70**, 3300–3316.
Meeks, J. C., Wolk, C. P., Schilling, N., Shaffer, P. W., Avissar, Y. & Chien, W.-S. 1978 *Pl. Physiol.* **61**, 980–983.
Miknis, F. P., Bartuska, V. J. & Maciel, G. E. 1979 *Am. Lab.*, Nov., pp. 19–33.
Pines, A., Gibby, M. G. & Waugh, J. S. 1973 *J. chem. Phys.* **59**, 569–590.
Preston, J. 1971 In *Kirk–Othmer encyclopedia of chemical technology* (ed. A. Standen), pp. 746–773. New York: Interscience.
Resing, H. A., Garroway, A. N. & Hazlett, R. N. 1978 *Fuel* **57**, 450–454.
Schaefer, J. & Stejskal, E. O. 1976 *J. Am. chem. Soc.* **98**, 1030–1032.
Schaefer, J., Kier, L. D. & Stejskal, E. O. 1980*c* *Pl. Physiol.* **65**, 254–259.
Schaefer, J., Sefcik, M. D., Stejskal, E. O. & McKay, R. A. 1979*b* *Polym. Prepr.* **20**, 247–250.
Schaefer, J., Sefcik, M. D., Stejskal, E. O. & McKay, R. A. 1980*b* Presented at the 21st Experimental NMR Conference, Tallahassee, Florida, March.
Schaefer, J., Sefcik, M. D., Stejskal, E. O., McKay, R. A. & Hall, P. L. 1980*a* Unpublished.
Schaefer, J., Stejskal, E. O. & Buchdahl, R. 1977 *Macromolecules* **10**, 384–405.
Schaefer, J., Stejskal, E. O. & McKay, R. A. 1979*a* *J. magn. Reson.* **34**, 443–447.
Schaefer, J., Stejskal, E. O. & McKay, R. A. 1979*c* *Biochem. biophys. Res. Commun.* **88**, 274–280.
Schaefer, J., Stejskal, E. O. & McKay, R. A. 1979*d* *J. magn. Reson.* **34**, 443–447.
Sefcik, M. D., Schaefer, J., Stejskal, E. O. & McKay, R. A. 1980 *Macromolecules* **13**, 1132–1137.
Sefcik, M. D., Stejskal, E. O., McKay, R. A. & Schaefer, J. 1979 *Macromolecules* **12**, 423–425.
Skokut, T. A., Varner, J. E., Schaefer, J., Stejskal, E. O. & McKay, R. A. 1979 *Pl. Physiol. Suppl.* **63**, 46.
Steger, T. R., Schaefer, J., Stejskal, E. O. & McKay, R. A. 1980 *Macromolecules* **13**, 1127–1131.
Stejskal, E. O., Schaefer, J. & Steger, T. R. 1979 *Faraday Symp. chem. Soc.* **13**, 56–62.
Stejskal, E. O., Schaefer, J. & Waugh, J. S. 1977 *J. magn. Reson.* **28**, 105–112.
Taki, T., Sogalse, T., Murphy, P. DuB. & Gerstein, B. C. 1980 Unpublished.
Tonelli, A. E. 1979 *Macromolecules* **12**, 255–256.
VanderHart, D. L. & Garroway, A. N. 1979 *J. chem. Phys.* **71**, 2772–2787.
VanderHart, D. L. & Retcofsky, H. L. 1976 *Fuel* **55**, 202–204.
Wignall, G. D., Child, H. R. & Li-Aravena, F. 1980 *Polymer* **21**, 131–132.
Wolk, C. P., Thomas, J., Shaffer, P. W., Austin, S. M. & Galonsky, A. 1976 *J. biol. Chem.* **251**, 5027–5034.
Wüthrich, H. 1976 In *NMR in biological research: peptides and proteins*, p. 307. Amsterdam: North-Holland.

Discussion

G. C. Levy (*Department of Chemistry, Florida State University, Tallahassee, U.S.A.*). Does Dr Schaefer have any idea of the lower limit for protons in organic solids, such as carbon fibre precursors, that will allow successful cross-polarization experiments? That quantity will, of course, have important implications for ^{13}C n.m.r. quantitative analysis in solids, particularly for heterogeneous samples.

J. Schaefer. If the protons are more or less uniformly distributed in a rigid organic solid, I suspect concentrations as low as 5% will generate cross-polarization spectra with representative carbon intensities. Naturally, one can imagine diabolical spatial distributions for which this would not be true. An accurate determination of the lower limit for protons requires a series of relaxation experiments. Similar cautions are appropriate if quantitative information is sought from heterogeneous samples in which various components have vastly differing motional properties, even though they may have comparable proton concentrations.

PHILOSOPHICAL TRANSACTIONS OF THE ROYAL SOCIETY A MATHEMATICAL, PHYSICAL & ENGINEERING SCIENCES